A General Perturbation Approach for Computational Fluid Dynamics

Leslie J. Chow* and Thomas H. Pulliam†
NASA Ames Research Center, Moffett Field, California

and

Joseph L. Steger‡
Stanford University, Stanford, California

An efficient numerical technique to produce accurate solutions to the equations of fluid dynamics is presented. The governing equations are perturbed about an approximate solution and solved by finite difference methods on a coarsened grid. This results in a scheme that substantially reduces the number of grid points necessary to resolve the flow accurately. Applications are presented for the two-dimensional Euler equations perturbed about solutions of the transonic full potential equation. However, the concept is applicable to arbitrary equation sets and higher dimensions and a wide variety of other applications.

I. Introduction

THE fundamental goal of computational fluid dynamics is to obtain solutions to the relevant flow equations quickly and inexpensively for application to problems of engineering interest. This objective can be met by using a variety of different approaches, each with inherent advantages and limitations. In finite difference simulations of steady-state flow, the governing equations are approximated by a large set of coupled nonlinear algebraic equations. These nonlinear equations are usually solved iteratively and require the use of large-scale computers.

To reduce the overall computational time and cost of obtaining finite difference solutions to a specified accuracy, several general strategies have been employed. The most common approach is to develop a more efficient iteration scheme that accelerates convergence to the correct steady-state solution. The second class of strategies consists of methods that simplify the equation set, i.e., restrict the range of application to certain flow conditions, such as irrotationality, or simplify the equation set locally (a zonal-type approach). The aim of the third class of methods is to reduce the number of points necessary to achieve a given accuracy. Methods of this type include higher-order schemes, such as spectral or high-order Padè methods and solution-adaptive grid techniques. The approach presented here belongs to this last class of methods, insofar as it employs a mechanism for reducing the number of computational points required to achieve a given accuracy.

Following a suggestion briefly outlined by Steger[1,2] and others,[3,4] an approximate base solution is embedded into the governing equation. The governing equation is then expressed in terms of a function that is smooth and gradually varying in regions where the base solution is an approximate or "nearby" solution. Such a function can be resolved with fewer grid points. A simple and readily solved equation set provides the base solution, which is required to be a good approximation over most of the flowfield.

Presented as Paper 83-1903 at the AIAA Sixth Computational Fluid Dynamics Conference, Danvers, Mass., July 13-15, 1983; received July 22, 1983; revision received March 25, 1984. This paper is declared a work of the U.S. Government and therefore is in the public domain.

*Research Scientist. Member AIAA.
†Research Scientist.
‡Associate Professor. Member AIAA.

In this paper, the perturbation method is applied to two-dimensional, steady, inviscid transonic airfoil calculations using the irrotational flow and Euler equations. However, the concept is applicable to arbitrary equation sets and higher dimensions, and it can be used in a wide variety of other applications. Moreover, traditional means of accelerating iterative convergence can still be used, and the perturbation terms appear to be readily embedded into any existing finite difference code.

Sections II and III detail the approach and numerical procedure. Steady transonic computations are presented and discussed in Sec. IV. Conclusions and possible extensions are contained in Sec. V.

II. Approach

Since a smooth, gradually varying function can be accurately resolved with fewer grid points than a rapidly varying one, the governing equations are reformulated to exploit this characteristic. The governing equation set is rewritten in terms of a perturbation about a known nearby or approximate base solution. The base solution should be one that is easily obtained and that is a good approximation over most of the flow domain. Thus, in most of the flow domain, the perturbation quantity (the difference between the two solutions) is a smooth, gradually varying function and the computational grid can be coarsened without appreciable loss of accuracy.

This concept is illustrated in Fig. 1, which shows the hypothetical Euler and full potential pressure distributions for two-dimensional transonic flow over the upper surface of an airfoil. For a strong shock case, the computed shock location differs, as does the predicted circulation. However, away from the shock region, the difference between the solutions is smooth and a coarse grid can be used for the perturbation form of the equations. Note that the solution itself can still change rapidly, especially at the airfoil nose. Thus, a coarse grid cannot be used for the unperturbed form of the governing equations.

The perturbation approach is outlined below for the steady two-dimensional Euler equations. The base solution is obtained from the irrotational flow equations.

Perturbation Euler Equations

The steady two-dimensional Euler equations in conservation law form can be expressed as

$$\partial_x E(Q) + \partial_y F(Q) = 0 \tag{1a}$$

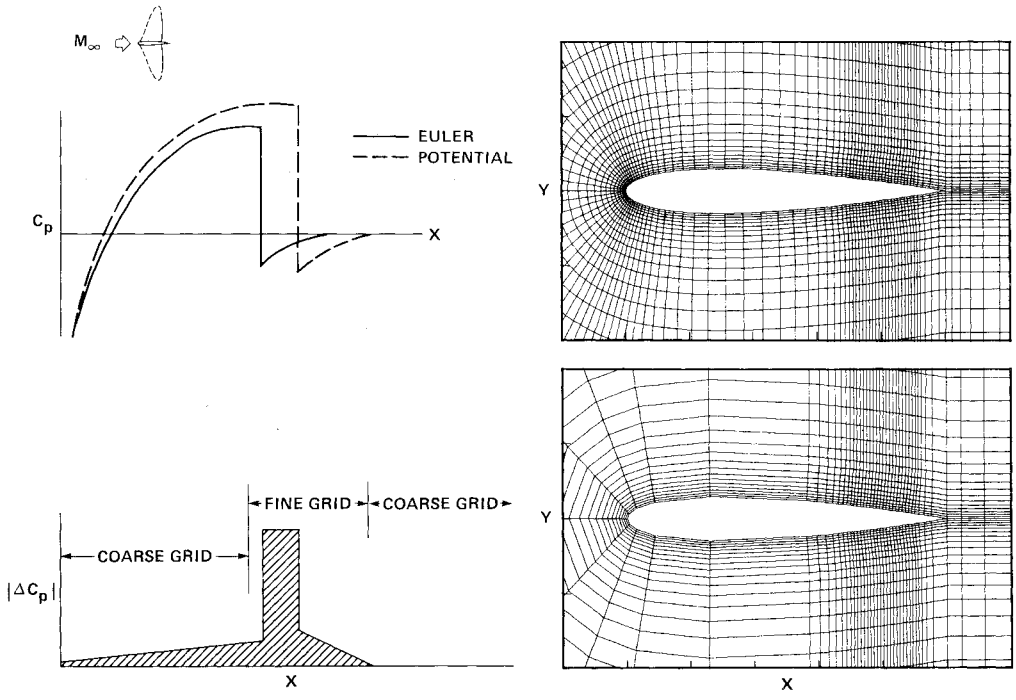

Fig. 1 Rationale behind perturbation approach (hypothetical Euler and full potential pressure distributions, computational grids).

where

$$Q=\begin{bmatrix}\rho\\ \rho u\\ \rho v\\ e\end{bmatrix},\quad E=\begin{bmatrix}\rho u\\ \rho u^2+p\\ \rho uv\\ u(e+p)\end{bmatrix},\quad F=\begin{bmatrix}\rho v\\ \rho uv\\ \rho v^2+p\\ v(e+p)\end{bmatrix} \tag{1b}$$

with pressure $p=(\gamma-1)[e-0.5\rho(u^2+v^2)]$ and ρ, u, v, and e are defined as the density, x- and y-direction velocity components, and total energy per unit volume, respectively.

For transonic flow, one can frequently assume that the shock waves are weak and treat the flow as irrotational and isentropic throughout. Then a velocity potential can be defined, which leads to a simplified equation set

$$\partial_x(\rho\phi_x)+\partial_y(\rho\phi_y)=0 \tag{2a}$$

$$\rho=\left[1-\frac{(\gamma-1)}{2}\left(\phi_x^2+\phi_y^2-1\right)\right]^{1/(\gamma-1)} \tag{2b}$$

For steady-state applications, very fast solution algorithms exist[5] for solving Eq. (2).

A solution of Eq. (2) is used to form a base solution for Eq. (1) as follows. By differencing ϕ we can form the elements of $Q_0=Q_0(\phi)$ from $u=\phi_x$, $v=\phi_y$, and the Bernoulli and isentropic relations. Thus, base solution flux terms $E_0=E_0(\phi)$ and $F_0=F_0(\phi)$ can be formed. In general, these flux terms do not satisfy the Euler equations and their boundary conditions. The potential solution is then embedded into Eq. (1) as

$$\partial_x E_0+\partial_y F_0+\left[\partial_x(E-E_0)+\partial_y(F-F_0)\right]=0 \tag{3}$$

Based on previous arguments, the flowfield can be discretized using a grid that is very coarse in regions where the quantities $(E-E_0)$ and $(F-F_0)$ are smooth. Equation (3) is then discretized as

$$\delta_x^f E_0+\delta_y^f F_0+\left[\delta_x^c(E-E_0)+\delta_y^c(F-F_0)\right]=0 \tag{4a}$$

The base solution is obtained on a fine grid and the partial derivatives are approximated with m-order-accurate finite difference formulas of the form

$$\delta_x^f=\partial_x+\mathcal{O}(\Delta x_f)^m \quad\text{and}\quad \delta_x^c=\partial_x+\mathcal{O}(\Delta x_c)^m \tag{4b}$$

where Δx_c is a grid spacing on the coarse grid and Δx_f a grid spacing on the fine grid.

In Eq. (4a) the flux derivatives are divided into two groups. The δ_x^f and δ_y^f terms represent the fluxes formed from the potential solution and finite differenced on a fine grid. The δ_x^c and δ_y^c terms represent a coarse-grid differencing of the perturbation fluxes. Note that Eq. (4a) is being solved on the coarse grid. Therefore, the fine-grid data from the base solution must be transferred to the coarse-grid points.

III. Numerical Algorithm

The perturbation scheme of Eq. (4) can be incorporated into existing computer codes with relative ease. From a coding standpoint, it is perhaps more convenient to view the scheme as the addition of a source term S_ϕ that corrects for the effects of grid coarseness. From this perspective, Eq. (4a) can be rewritten as

$$\delta_x^c E+\delta_y^c F=-S^f+S^c\equiv S_\phi \tag{5a}$$

where

$$S^f\equiv\delta_x^f E_0+\delta_y^f F_0 \quad\text{and}\quad S^c\equiv\delta_x^c E_0+\delta_y^c F_0 \tag{5b}$$

The modification of existing codes requires only the addition of the term S_ϕ.

The implicit approximate factorization scheme[9] used for solving the Euler equations in this application is

$$\left[I+h\delta_x A^n\right]\left[I+h\delta_y B^n\right]\Delta Q^n=-h\left[\delta_x E^n+\delta_y F^n\right] \tag{6}$$

where $A=\partial E/\partial Q$ and $B=\partial F/\partial Q$ are the flux Jacobians, h the time step, and $\Delta Q^n=Q^{n+1}-Q^n$.

In lieu of solving Eq. (6) on a fine grid, S_ϕ is added to the right-hand side and the following equation is solved on a

coarse grid:

$$\left[I + h\delta_x^c A^n\right]\left[I + h\delta_y^c B^n\right]\Delta Q^n = -h\left[\delta_x^c E^n + \delta_y^c F^n - S_\phi\right] \quad (7)$$

For a steady-state calculation, the source term is computed only once and it remains fixed throughout the computation. Additional storage is required for the source term; but, because of the reduced number of grid points, all arrays required by the original algorithm are reduced in size. The net effect is a substantial reduction in storage requirements.

The Finite Difference Operators

The perturbation solution is computed on a coarse grid. Therefore, the fine-grid data S^f must be transferred to the coarse grid by some "restriction" process.

Define I_f^c as a restriction operator that transfers the fine-grid data onto the coarse-grid points. (Notation similar to that of multigrid techniques is adopted.[6]) This can be accomplished by interpolation if the coarse-grid points are not coincident with fine-grid points or by "injection" when the coarse-grid points do coincide with fine-grid points.

The difference operators of Eq. (4b) are then defined as

$$\delta_x^f E_0 = I_f^c \delta_x E_0(Q_0) \quad \text{and} \quad \delta_x^c E_0 = \delta_x E_0\left(I_f^c Q_0\right) \quad (8)$$

where δ_x without a superscript is an arbitrary finite difference operator. Note that when the fine and coarse grids are identical, $\delta_x^f E_0$ is equal to $\delta_x^c E_0$. The operators δ_y^f and δ_y^c are defined analogously.

Restriction Operator, I_f^c

Injection Case

A coarse grid can easily be formed by discarding points of the fine grid that was used to compute the potential solution. Then all coarse-grid points are coincident with the fine-grid points and the restriction operation consists of repacking the fine-grid data set so that only the data associated with the coincident points are retained. A "clustered" grid can easily be formed by retaining most or all of the fine-grid points in selected regions. Note that in local regions where the fine and coarse grids are identical (i.e., no nearby points have been discarded), the term S^f is equal to the term S^c so that the source term S_ϕ is locally zero and Eq. (4) reverts back to the standard unperturbed finite difference scheme [Eq. (6)]. This local cancellation is convenient since, in regions where high resolution is desirable (for instance, in shock regions), the base solution may no longer be a nearby solution for the Euler equations. In this way, the standard Euler equation is solved locally.

Interpolation Case

When the coarse-grid points are not coincident with the fine-grid points, the fine-grid data are interpolated onto the coarse-grid points. The interpolation scheme used here is a two-dimensional, second-order-accurate Taylor series expansion. Since the coarse-grid points do not coincide with fine-grid points, the S^f and S^c components of the source term are not equal to each other. Unlike the injection case, the forcing function S_ϕ is nonzero in the entire flowfield, including the fine-grid regions. To obtain a Euler calculation in the vicinity of a shock, the forcing function is set to zero locally. This region can be chosen somewhat arbitrarily. The perturbation solution is relatively insensitive to variation in the extent of this region as long as it contains both the isentropic and the Euler shocks. With the base solution in hand, the location of this region is known. This region could be located automatically by monitoring entropy production in the flowfield.

Generalized Coordinates

The perturbation procedure has been applied to the Euler equations in generalized curvilinear coordinates. The perturbation source term is embedded into a finite difference code that solves the conventional two-dimensional Euler equations in general curvilinear coordinates.[7-10]

The parent code uses an implicit approximate factorization algorithm in delta form,[9]

$$L_\xi L_\eta \Delta\hat{Q}^n = -hL_R\hat{Q}^n \quad (9)$$

where

$$L_\xi = \left[I + h\delta_\xi \hat{A}^n - \epsilon_i \Delta t J^{-1}\nabla_\xi \Delta_\xi J\right]$$

$$L_\eta = \left[I + h\delta_\eta \hat{B}^n - \epsilon_i \Delta t J^{-1}\nabla_\eta \Delta_\eta J\right]$$

$$L_R\hat{Q}^n = \left[\delta_\xi\left(\hat{E}(\hat{Q}^n)\right) + \delta_\eta\left(\hat{F}(\hat{Q}^n)\right)\right]$$

$$-\epsilon_e J^{-1}[(\nabla_\xi\Delta_\xi)^2 + (\nabla_\eta\Delta_\eta)^2]J\hat{Q}^n$$

and where $h = \Delta t$ for first-order accuracy in time, $\hat{Q}$, $\hat{E}$, $\hat{F}$ are transformed vectors, and ϵ_i and ϵ_e are implicit and explicit dissipation coefficients.

The source terms defined in Eq. (5) are written in transformed coordinates and added to the right-hand side of Eq. (9). Some care must be taken to scale the forcing terms by the appropriate metric terms. The coarse-grid component of the forcing function $\hat{S}^c$ is scaled by the coarse-grid Jacobian. The fine-grid component of the forcing function $\hat{S}^f$ is scaled by a restricted fine-grid Jacobian. In interpolation cases, the restricted fine-grid Jacobian of Eq. (10b) was approximated by the coarse-grid Jacobian. In particular, the source term S_ϕ becomes $\hat{S}_\phi = \hat{S}^c - \hat{S}^f$ with

$$\hat{S}^c = L_R\hat{Q}_0^c = \delta_\xi^c\hat{E}_0\left(\hat{Q}_0^c\right) + \delta_\eta^c\hat{F}_0\left(\hat{Q}_0^c\right)$$

$$-\epsilon_e\left[\left(\nabla_\xi^c\Delta_\xi^c\right)^2 + \left(\nabla_\eta^c\Delta_\eta^c\right)^2\right]\hat{Q}_0^c \quad (10a)$$

$$\hat{S}^f = \left(J_f^c\right)^{-1} I_f^c\left[J_f L_R\hat{Q}_0\right]$$

$$= \left(J_f^c\right)^{-1} I_f^c\left\{J_f\left(\delta_\xi^f\hat{E}_0(\hat{Q}_0) + \delta_\eta^f\hat{F}_0(\hat{Q}_0)\right.\right.$$

$$\left.\left.-\epsilon_e\left[\left(\nabla_\xi^f\Delta_\xi^f\right)^2 + \left(\nabla_\eta^f\Delta_\eta^f\right)^2\right]\hat{Q}_0\right)\right\} \quad (10b)$$

where $\hat{Q}_0^c = J_c^{-1} I_f^c (J_f\hat{Q}_0)$ and $J_f^c = I_f^c J_f$. Thus, the perturbation Euler algorithm that replaces Eq. (9) is given by

$$L_\xi L_\eta \Delta\hat{Q}^n = -h\left[L_R\hat{Q}^n - \hat{S}_\phi\right] \quad (11)$$

IV. Results and Discussion

The perturbation Euler scheme of Eq. (11) is solved using a fully conservative irrotational base solution. The irrotational code is written in terms of the primitive variables. It is chosen for use here, because it is directly compatable with the Euler code. A full potential code such as TAIR[3] would have run considerably faster.

The computations used a spatially varying time step where $\Delta t_{j,k} = \Delta t_0/(1 + \sqrt{J_{j,k}})$ and with an explicit smoothing coefficient of 2. The residual is defined to be the right-hand side of Eq. (9) divided by $\Delta t_{j,k}$. Acceptable convergence (a drop in

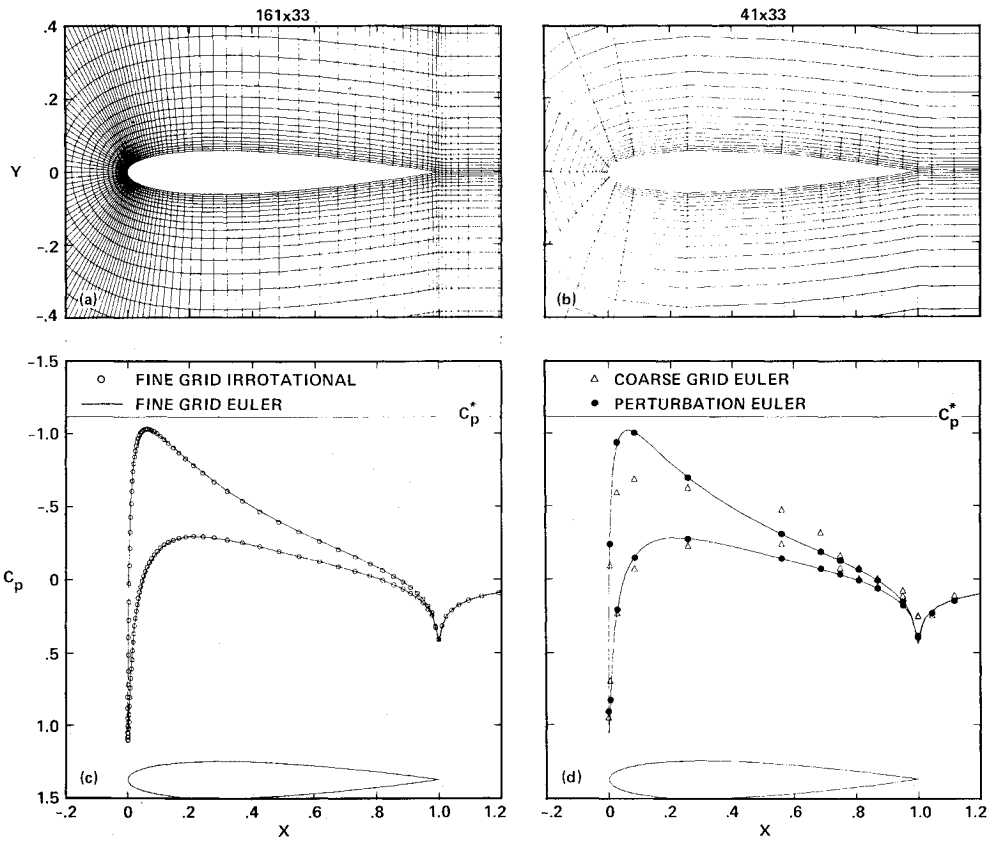

Fig. 2 Subcritical lifting NACA 0012 case ($M_\infty = 0.63$, $\alpha = 2$ deg): a) fine grid; b) fine-grid surface pressure coefficients, Euler solution vs irrotational solution; c) coarse grid; d) coarse-grid Euler and perturbation Euler solutions.

the residual of 2.5-3 orders of magnitude) is obtained in 300 time steps. The fine-grid potential solution is restricted to the coarse grid and used as initial conditions for all coarse-grid cases. (Freestream initial conditions were also tested. No discernable differences in convergence rate or solution were found.) For comparison purposes, fine-grid Euler solutions were also generated. These reference solutions were computed on the same fine grids used to obtain the base solutions. The grids are generated by an algebraic grid generator[8] and all computations were run on a CDC 7600 computer.

Subcritical Lifting NACA 0012 Case

As a necessary check of the perturbation procedure, a subcritical inviscid flow solution was obtained for a lifting airfoil. For a uniform freestream, this flow is irrotational, so the approximate base solution is also the solution of the Euler equation. The irrotational base solution for a NACA 0012 airfoil at an angle of attack α of 2 deg and a freestream Mach number M_∞ of 0.63 was computed on the fine mesh shown in Fig. 2a. The mesh contains 161 points in the streamwise ξ direction and 33 points in the near normal η direction. Surface pressure coefficients for the fine-grid irrotational and Euler solutions are presented in Fig. 2b. As expected for this subcritical case, the Euler and irrotational solution are virtually identical.

The coarse grid of 41×33 points shown in Fig. 2c was used to compute coarse-grid Euler and perturbation Euler solutions. Figure 2d shows the coarse- and fine-grid Euler solutions of Eq. (9). It is clear that the grid coarseness gives rise to unacceptable inaccuracies. A coarse-grid perturbation Euler solution was computed using the interpolation restriction operator. The forcing function is nonzero in the entire domain. The perturbation solution is compared with the fine-grid Euler calculation in Fig. 2d and shows excellent agreement. Comparison of interior flowfield data, such as contour plots of Mach number or pressure, substantiate the accuracy of the computations.

Transonic Nonlifting NACA 0012 Case

As a true test of the perturbation procedure, a transonic rotational case was calculated. The fine-grid base solution was computed on the 161×33 clustered mesh shown in Fig. 3a. The flowfield conditions are $M_\infty = 0.85$ and $\alpha = 0.0$ deg. The irrotational solution is compared with a fine-grid Euler solution in Fig. 3b. As is typical for this Mach number range, the irrotational solution overpredicts the shock strength and places the shock about 10% of chord downstream of the Euler shock.

The 91×29 point coarse grid shown in Fig. 3c was used to obtain a perturbation Euler solution. Since the coarse-grid points do not coincide with the fine-grid points, the interpolation restriction operator must be used and the source terms are nonzero in the entire domain. To obtain a Euler solution in the shock region, S_ϕ is set to zero from about 57% of chord to the trailing edge, as shown by the shaded region in Fig. 3c. The perturbation solution is compared with fine- and coarse-grid Euler solutions in Fig. 3d. The perturbation Euler solution shows excellent agreement with the fine-grid Euler solution. Comparison of the interior data also exhibits excellent flowfield agreement.

Transonic Lifting NACA 0012 Case

A fine-grid base solution was computed for a NACA 0012 airfoil at $M_\infty = 0.8$ and $\alpha = 1.0$ deg. The 161×33 point computational grid is shown in Fig. 4a. Pressure coefficients for the irrotational solution are compared with a fine-grid Euler solution in Fig. 4b. Both equation sets predict a strong shock on the upper surface with the expected discrepancy in shock location.

An injection coarse grid of 69×33 points was used to compute Euler and perturbation Euler solutions. The coarse grid is identical to the fine grid in the shaded region shown in Fig. 4c. Figure 4d shows that the coarse-grid Euler solution incorrectly predicts the lower surface shock location and underpredicts the upper surface shock strength. The coarse-grid perturbation solution is in very good agreement with the

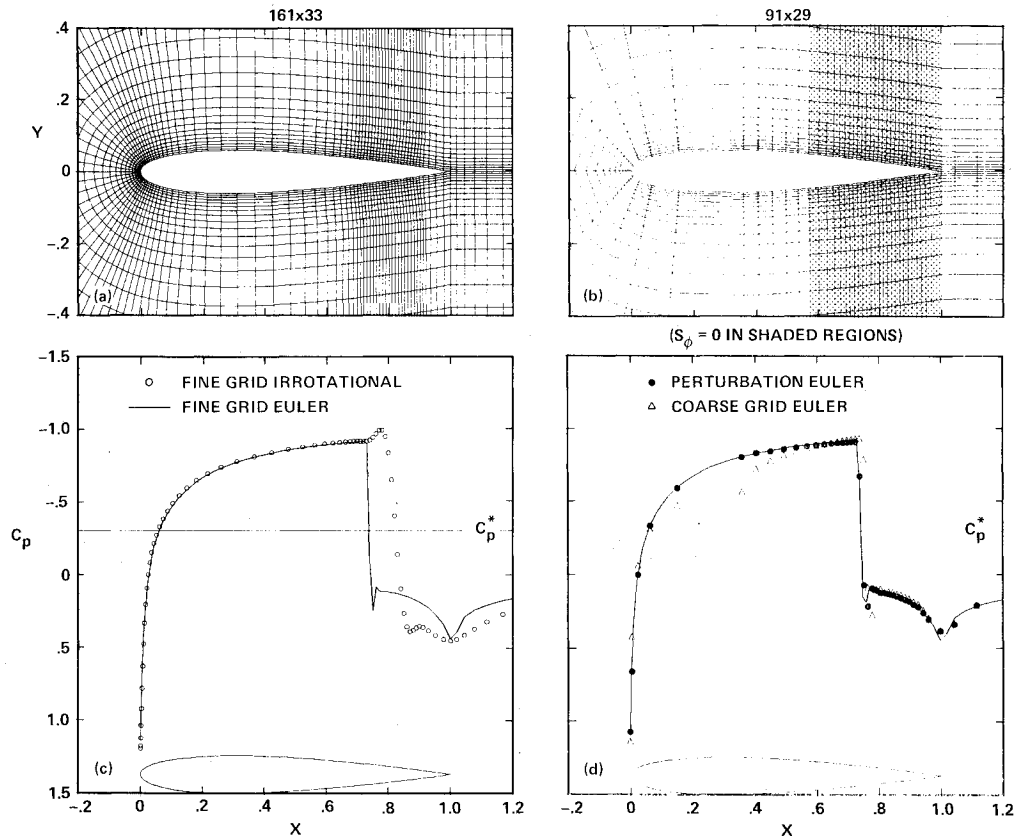

Fig. 3 Transonic nonlifting NACA 0012 case ($M_\infty = 0.85$, $\alpha = 0$ deg): a) fine grid; b) fine-grid surface pressure coefficients, Euler vs irrotational solutions; c) coarse grid, $S_\phi = 0.0$ in shaded region; d) coarse-grid Euler and perturbation Euler solutions.

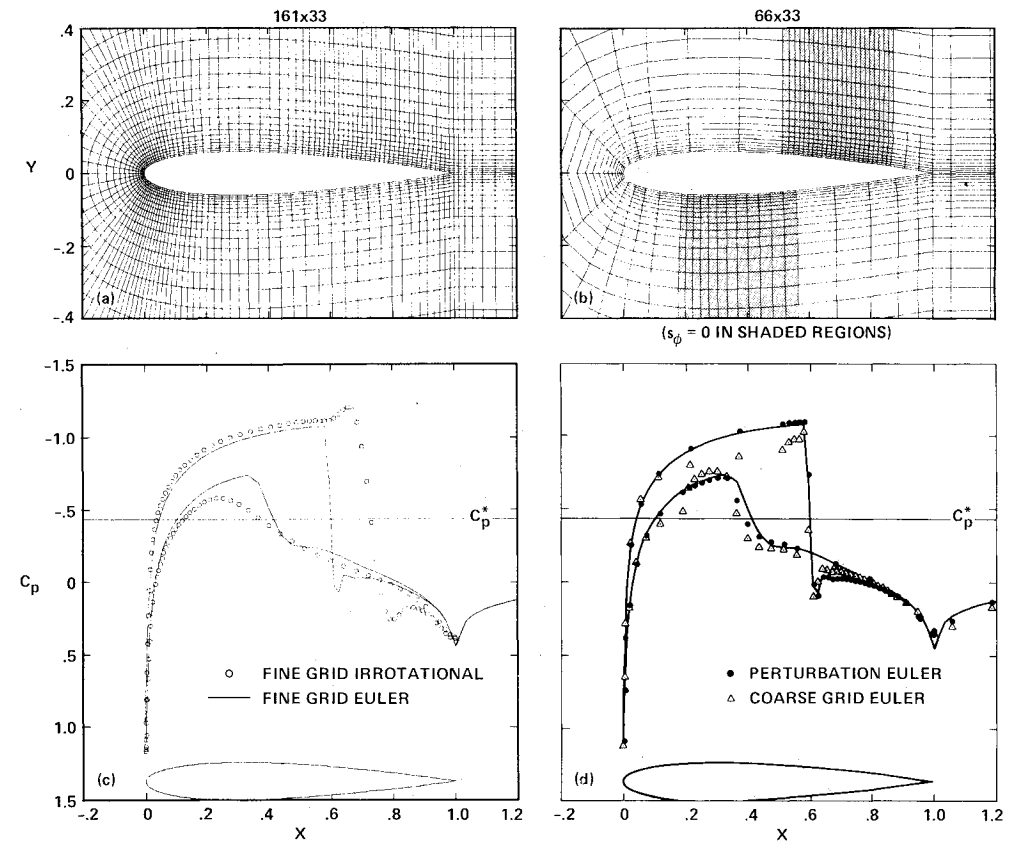

Fig. 4 Transonic lifting NACA 0012 case ($M_\infty = 0.80$, $\alpha = 1$ deg): a) fine grid; b) fine-grid surface pressure coefficients, Euler solution vs irrotational solution; c) coarse grid, $S_\phi = 0.0$ in shaded region; d) coarse-grid Euler and perturbation Euler solutions.

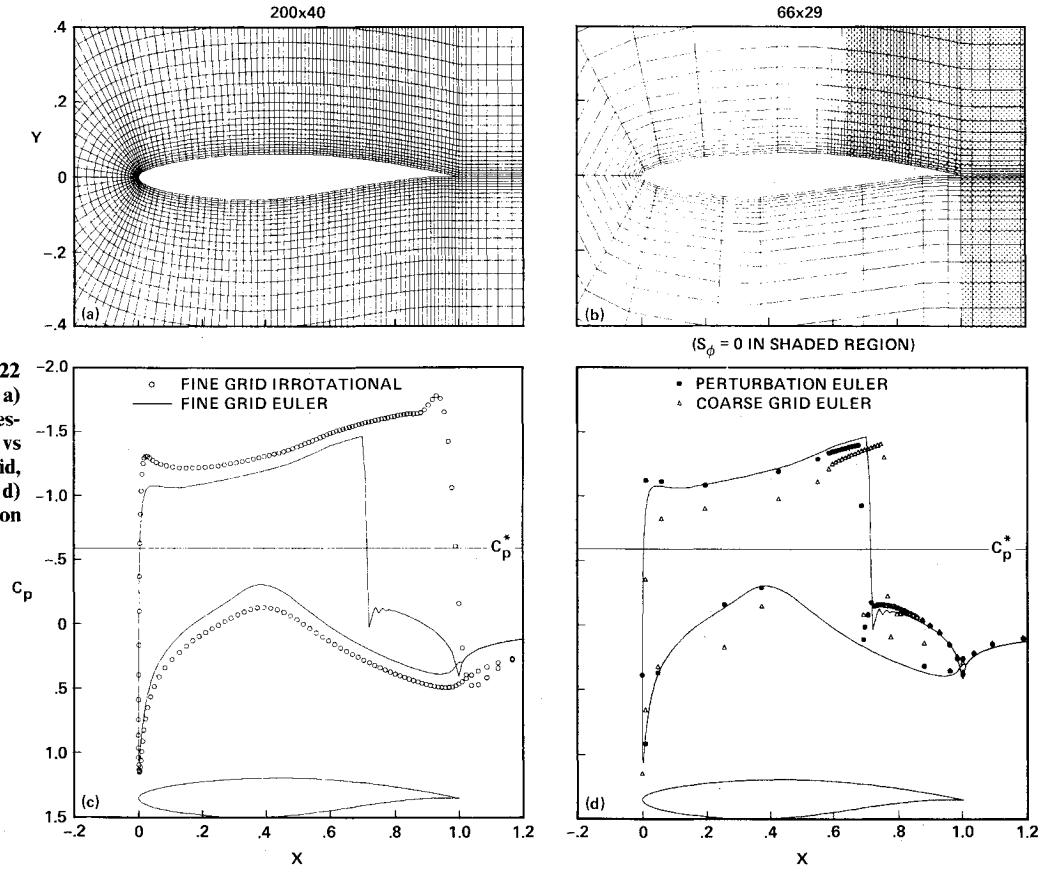

Fig. 5 Transonic lifting RAE 2822 case ($M_\infty = 0.75$, $\alpha = 3$ deg): a) fine grid; b) fine-grid surface pressure coefficients, Euler solution vs irrotational solution; c) coarse grid, $S_\phi = 0.0$ in shaded region; d) coarse-grid Euler and perturbation Euler solutions.

fine-grid Euler solution and, as before, the interior solution also exhibits good accuracy.

Transonic Lifting RAE 2822 Case

In a similar fashion, a perturbation computation was run for a lifting transonic RAE 2822 airfoil at $M_\infty = 0.75$ and $\alpha = 3$ deg. The fine grid is shown in Fig. 5a. The C_p distribution predicted by the irrotational solution is compared with the fine-grid Euler distribution in Fig. 5b. Note that the computed base solution has an overshoot near the leading edge, while the fine-grid Euler does not. This is a more stringent test of the method because of the rapid expansion at the leading edge and the grossly inaccurate location of the irrotational shock at the trailing edge.

The 66×29 point coarse grid is shown in Fig. 5c. The perturbation source term was restricted in both the ξ and η directions by interpolation and set to zero in the shaded region in Fig. 5c. The perturbation formulation gives a considerable improvement over the standard formulation, but overpredicts the leading-edge expansion and places the shock 2.5% upstream of the fine-grid Euler shock. (See Fig. 5d.) This result underscores the relationship between the quality of the base solution and the quality of the perturbation solution. The perturbation formulation yields an improvement over the standard formulation on a coarse grid, if the base solution is a "good" approximation to the fine-grid Euler solution over most of the domain. Since the perturbation source term supplies gradient information, the effect of an overshoot in the base solution is amplified and the perturbation solution may show some degradation in that region. Similarly, if the gradient of the base solution is of the wrong sign, it is reflected in the perturbation solution by a local decrease in accuracy. In this case, the information supplied by the base solution is driving the perturbation solution to an inaccurate leading-edge expansion, which in turn leads to a less accurate shock location.

Even so, the perturbation solution compares favorably with the fine-grid Euler solution.

Summary of Results

In summary, the perturbation Euler solutions were able to accurately capture steady, two-dimensional transonic solutions on very coarse grids. The addition of the potential source term was able to alleviate or eliminate the effect of grid coarseness in the perturbation Euler computations. For 300 time steps on a CDC 7600 computer, fine-grid Euler computations required between 680 and 1025 s while perturbation Euler computations required between 175 and 400 s.

V. Conclusions

The perturbation scheme has been applied for steady, inviscid transonic solutions of the two-dimensional Euler equations using a conservative irrotational base solution. This scheme is able to accurately resolve the flowfield on a coarse mesh for which the standard Euler algorithm produces an unacceptable solution. The perturbation Euler scheme reduced the computation time by a factor of 2-4 and produced a net reduction in array storage of 26-70% over that of the fine-grid Euler calculation. The perturbation scheme is easily embedded into existing codes by the addition of a simple source term and traditional means of accelerating iterative convergence can still be used.

The perturbation scheme could be used in a design cycle, where potential solutions are generated routinely, and the Euler perturbation method could be used as a second-cut analysis. However, the concept has much broader implications. Other equation sets could be coupled; for instance, the Navier-Stokes equations could be perturbed about a full potential/boundary-layer solution. Extension to three dimensions would compound the reduction in computation time. The perturbation scheme could also be developed for a patch-

type mesh. In this instance, a fine-grid patch could be embedded into a grid that is very coarse in both the streamwise and nearly normal directions, thus increasing computational savings. Application of the perturbation scheme has yielded promising results for the Euler/full potential coupling.

References

[1]Steger, J.L., "A Computer Program for the Internal Flow of Spin-Stabilized Liquid-Filled Shells," Flow Simulations Contract Rept. 79-03, submitted to ARRADCOM, Oct. 1979.

[2]Steger, J.L., "On Application of Body Conforming Curvilinear Grids for Finite Difference Solution of External Flow," *Numerical Grid Generation*, edited by J.F. Thompson, North-Holland Publishing Co., New York, 1982, pp. 295-316.

[3]Buning, P.G. and Steger, J.L., "Solution of the Two-Dimensional Euler Equations with Generalized Coordinate Transformations Using Flux Vector Splitting," AIAA Paper 82-0971, June 1982.

[4]Israeli, M. and Ungarish, M., "Improvement of Numerical Solutions by Incorporation of Approximate Solutions Applied to Rotating Compressible Flows," *Proceedings, Seventh International Conference on Numerical Methods in Fluid Dynamics*, edited by W.C. Reynolds, and R.W. MacCormack, Springer-Verlag, New York, 1980, pp. 230-235.

[5]Holst, T.L., "Numerical Computation of Transonic Flow Governed by the Full Potential Equation," *VKI Lecture Series on Computational Fluid Dynamics*, von Kármán Institute, Rhode-St-Genese, Belgium, March 1983.

[6]Brandt, A., "Multilevel Solutions to Boundary Value Problems," *Mathematics of Computation*, Vol. 31, 1977, pp. 333-390.

[7]Steger, J.L., "Implicit Finite-Difference Simulation of Flow About Arbitrary Two-Dimensional Geometries," *AIAA Journal*, Vol. 16, 1978, pp. 679-686.

[8]Pulliam, T.H., Jespersen, D.C., and Childs, R.E., "An Enhanced Version of an Implicit Code for the Euler Equations," AIAA Paper 83-0344, Jan. 1983.

[9]Beam, R.M. and Warming, R.F., "An Implicit Finite-Difference Algorithm for Hyperbolic Systems in Conservation-Law-Form," *Journal of Computational Physics*, Vol. 22, 1976, pp. 87-110.

[10]Warming, R.F. and Beam, R.M., "Upwind Second-Order Difference Schemes and Applications in Aerodynamic Flows," *AIAA Journal*, Vol. 14, 1976, pp. 1241-1249.